

**ELECTRONIC AND STRUCTURAL PROPERTIES  
OF  
FERROMAGNETIC SHAPE MEMORY ALLOYS**

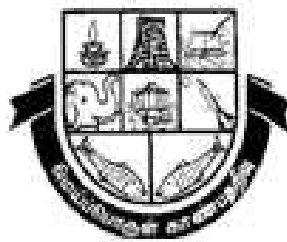
**A SYNOPSIS**

*Submitted by*

**R. Shanmugasundari**

*In fulfilment for the Award of the Degree of*

**DOCTOR OF PHILOSOPHY**



**MADURAIKAMARAJUNIVERSITY**

**MADURAI – 625 021**

**INDIA.**

**2012**

# Chapter 1

## Introduction

Shape Memory Alloy (SMA) is a novel material having the ability to return to the predetermined shape when heated. Generally, they can be deformed at some relatively low temperature and upon exposure to high temperature they will regain their shape prior to deformation. This effect relies on two deformation mechanisms, phase transformation and twin boundary motion. The phase transition in a SMA is from a high temperature phase called austenite to a low temperature, lower symmetry phase called martensite.

In Ferromagnetic Shape Memory Alloy (FSMA), the deformation of the martensite phase is actuated by the application of magnetic field. The applied field interacts with the crystal's magnetic moments that are coupled to the crystal structure. FSMAs are capable of producing higher strains at frequencies of the order of 1 kHz [1-4]. FSMA Ni-Mn-Ga is representative of the family of the Heusler type alloys, which exhibit both martensitic transformation temperature and Curie temperature. Robert C. O' Handley and his co-workers at Massachusetts Institute of Technology [5-10] first reported Magnetic-Field- Induced Strains (MFIS) of nearly 0.2% in unstressed crystals of Ni-Mn-Ga under magnetic fields of 8 kOe applied at 265 K. Widespread research was then carried out to investigate the properties and MFIS in Ni-Mn-Ga system and other alloys. The other interesting FSMAs are Ni-Mn-Ga, Ni-Mn-Al, [11], Ni-Mn-Ga-Co [12], Co-Mn-Ga, Fe-Co-Ga and Ni-Mn-Sn [13].

Certain material properties are needed for FSMA [13] to exhibit field-induced strain. High magneto crystalline anisotropy is essential because magnetization rotation within the unit cell is an alternate process to twin motion. If magnetization rotation can happen at low field, it will be favoured and twin boundary motion will be less likely. Low yield stress in the martensite allows the magnetic driving forces to move the twin boundaries easily and cause the material to strain. High yield stresses in the material implies that larger fields will be required to actuate a given strain and the strain versus field hysteresis will be greater. Finally, high saturation magnetization in

the presence of an applied field will provide the driving force necessary to perform work with the material [13].

### 1.1 Previous work on Ni-Mn-Ga

Extensive research was carried out to examine the FSMA properties in Ni-Mn-Ga system. By tuning the proportion of the Ni, Mn and Ga in the alloy, it is possible to increase the electron to atom ratio, which increases the martensitic transition temperature from 220K in stoichiometric Ni-Mn-Ga so that the FSMA material can work at room temperature. On cooling below 202 K, Ni-Mn-Ga undergoes a martensitic phase transformation to a tetragonal structure with  $c/a < 1$  [14]. The most important experimental results on crystal structure, magnetic anisotropy and twinning stress of martensitic phases in Ni-Mn-Ga having tetragonal five layered, orthorhombic seven layered and tetragonal non-layered crystal structures were reported by Ullakko et al [15].

Widespread study of the temperature dependencies of resistivity of several Ni-Mn-Ga and Ni-Fe-Ga alloys and the magnetic-field influence on the martensitic transformation temperatures were carried out by Barandiaran et al [16]. They have reported an existence of low-field minimum of the martensitic transformation temperature for single and polycrystalline Ni-Mn-Ga alloys.

Single crystal of a tetragonally distorted Heusler alloy in the Ni-Mn-Ga system has shown a 6 % shear strain at room temperature in a field of 4 kOe [17]. The field-induced strains occur at smaller fields as the stress required nucleating twin boundary motion, decreases. Decreased magneto-crystalline anisotropy or increased external stress limits the magnitude of the field-induced strains. The alloy is found to have low hysteresis, large strains ~up to 10%, and a transition temperature that is adjustable with composition [18]. Lot of studies on Ni-Mn-Ga that results in large MFIS were reported [19-23].

Major features of stress-strain-temperature behaviour experimentally observed in Ni-Mn-Ga were explained using a model based on the statistical description of martensite nucleation events by Chernenko et al [24]. The compressive stress-strain superelastic behaviour of austenite at different temperatures and strain

rates had been studied for a single crystalline  $\text{Ni}_{49.4}\text{Mn}_{27.7}\text{Ga}_{22.9}$  alloy using a ZWICK-100 testing machine.

Extensive experimental studies were carried out by many researchers for structure determination and performance of these alloys. The martensitic transformation and the magnetic properties of the alloys were found to depend strongly on Mn/Ga ratio and on the annealing temperature [25, 26]. With increase in Mn substitution for Ga, martensite transformation temperature increased, while the curie temperature and magnetization values decreased [27]. This was attributed to the e/a ratio of the alloys.

The mechanisms of the magnetic micro structure, which cause the martensite band domains to run diagonally in a micrograph from left to right was observed [28]. Martensitic transformation of Ni–24.7Mn–24.8 Ga (at.%) alloy not only depend on the structural rearrangement but was also found to respond to magnetic field.

Awaji et al [29] carried out experiments in a broader temperature range using high magnetic field and reported martensitic transition temperature increase and pre-martensitic transition temperature decrease with application of magnetic fields up to 2 T. The transition temperatures do not change in fields up to 5 T [29].

Wedel et al [30] proposed a new model for the tetragonal compound Ni-Mn-Ga and the non-stoichiometric phases with the help of TEM, XRD data, and a computational simulation based on the XRD patterns. The results of the observations in the study had shown that Ni-Mn-Ga and the corresponding non-stoichiometric Ni-rich alloys at low temperature have a tetragonal crystal structure.

Measurements of the temperature dependencies of resistivity under constant magnetic fields by Barandiaran et al. [31] made it possible to clarify the premartensitic transition sensitivity to applied magnetic field up to 14 Tesla in polycrystalline and mono crystalline Ni–Mn–Ga alloys with compositions close to the stoichiometric one. Studies about crystal structure, preferential site occupancy, variant reorientation and magnetic moment distribution in FSMA was reported by Barandiaran et al [32].

Structural properties of magnetic Heusler alloys with composition  $X_2YM$  were studied by Ayuela et al., [13] within the Density-Functional Theory (DFT) with the Generalized Gradient Approximation (GGA) for the electronic exchange and correlation. The structures and magnetic moments at equilibrium were found to be in good agreement with the values. They studied Heusler alloys based on the  $X_2YM$  stoichiometry for the  $L2_1$  and distorted phases:  $Ni_2MnM$  with  $M = Al, Ga, Sn$ , and the compounds  $Co_2MnGa$ ,  $Ni_2CoGa$ , and  $Fe_2CoGa$ . They made the study using the Full-Potential Linearized Augmented-Plane-Wave (FLAPW) method, using a non-local approximation for the exchange and correlation potential.

Ozdemir Kartet al [33] carried out spin-polarized total energy calculations for Ni-Mn-Ga by using Vienna Ab Initio Simulation Package (VASP) and the implemented Projector Augmented Wave Pseudo Potential Formalism (PAW) and reported  $a=5.812 \text{ \AA}$ . In their work, a detailed study of structure, magnetic and mechanical properties of Ni-Mn-Ga were performed using DFT.

Ayela et al. [34] reported studies of the variants of Ni-Mn-Ga alloys, in particular the tetragonal structures with  $c/a < 1$  from the theoretical point of view, using the GGA FLAPW method. The effective value of the DOS splitting was proportional to the deformation. In line with the results the electronic density was also examined and found to be in agreement with the neutron scattering experiments.

Breczko et al [35] presented results of the computer simulations and experimental investigation of physical properties of Ni-Mn-Ga alloy. Simulation of atomic clusters were done using NWChem package.

## **1.2 Applications of FSMA**

The unique combination of high strains, high actuation frequency and large energy densities make these materials promising for a variety of military and civilian applications. Potential applications include devices for vibration and signature control, energy harvesting, novel aerodynamic and hydrodynamic control systems, active shock amelioration systems and sonar devices.

### **1.2.1 Actuators**

The main application of magnetic shape memory alloys is as actuators. Compared to conventional actuator technologies (hydraulics, solenoid and pneumatics), the advantages include fast response, reduced size, reliability and efficiency [36].

### **1.2.2 Sensors**

The inverse application of the MSM property is used for sensing. The larger variation of magnetic flux density is caused when the MSM is mechanically compressed in testing device. The variation of magnetic flux density depends on the geometrical and material parameters of the MSM element, as well as on its deformation rate [37].

### **1.2.3 Energy Harvesters and Absorbers**

The change in the flux density induced by external stress can be further extended to voltage generation and energy harvesting. Energy harvesters provide a very small amount of power for low-energy electronics. They act as power sources that convert vibrations and rotation into energy. They operate wireless sensors without batteries [38].

The Ni-Mn-Ga/PU polymer composite was shown to be ideal for applications that require absorption of mechanical energy in 2008 by Mahendran et al. [39]. David C. Dunand and Peter Müllner [40] reviewed processing, micro and macrostructure, and magneto-mechanical properties of Ni-Mn-Ga powders, fibres, ribbons and films with one or more small dimension, which are amenable to the growth of bamboo grains leading to large MFIS. They experimented on “constructs” from these structural elements (e.g., mats, laminates, textiles, foams and composites). MFIS are very large (up to 10%) for mono crystalline Ni-Mn-Ga, they are near zero (<0.01%) in fine-grained poly crystals due to incompatibilities during twinning of neighbouring grains and the resulting internal geometrical constraints. By growing the grains and/or shrinking the sample, the grain size becomes comparable to one or more characteristic

sample sizes (film thickness, wire, ribbon width, particle diameter, etc.), and the grains become surrounded by free space. This reduces the incompatibilities between neighbouring grains and can favour twinning and thus increase the MFIS. This approach was validated by them [40] recently with very large MFIS (0.2 to 8%) measured in Ni-Mn-Ga fibres and foams with bamboo grains with dimensions similar to the fibre and in thin plates where grain diameters are comparable to plate thickness.

### **1.3 Scope of the Thesis**

The study intend exploring the power of Gaussian to find Molecular energies, Structures of transition states, Molecular orbitals, Vibrational frequencies and prediction of NMR properties of Ni-Mn-Ga. The second part of this work aims at the investigation of magnetic properties of Ni-Mn-Ga through experimental procedures. This effort is a seminal approach to study the properties of Ni-Mn-Ga using Gaussian, though it posed a lot of challenges. Owing to the greater size of the system, computing time in high speed workstations was at least thirty hours or more for a single Gaussian job. We are forced to be contented with single point energy calculations since achieving convergence was quite difficult.

### **1.4 Organisation of the Thesis**

In the thesis, introduction about FSMA and research in particular to Ni-Mn-Ga are given in chapter 1. Computational methods and the basic information about the tools used in the study are explained in Chapter 2. Theoretical study of austenite Ni-Mn-Ga using Gaussian and prediction of electronic and structural properties are elucidated in Chapter 3. The similar study for both orthorhombic and tetragonal martensite of Ni-Mn-Ga is detailed in Chapter 4. Observations from experimental procedures to find magneto-mechanical properties of polycrystalline Ni-Mn-Ga FSMA are elaborated in chapter 5 and the last unit details about results, discussion and future scope for further research.

## Chapter 2

### Computational Methods

Computational Analysis can also be described as science performed using computers rather than chemicals. *Ab initio* mean “from the beginning” or “from first principles” using laws of quantum mechanics. Over the last two decades powerful molecular modelling tools have been developed which are capable of accurately predicting structures, energetics, reactivities and other properties of molecules. These developments are largely due to the design of efficient quantum chemical algorithms. In our study about Ni-Mn-Ga, both Hartree–Fock (HF) and Density Functional Theory (DFT) algorithms are being used. Hartree-Fock theory is a wave function-based approach that relies on the mean-field approximation. Density Functional Theory methods obtain the energy from the electron density rather than the complicated wave function.

#### 2.1 Hartree-Fock Theory

In computational physics, the HF method [41] is an approximate method for the determination of the ground-state wave function and ground-state energy of a quantum many-body system. HF theory is fundamental to electronic structure theory, which uses a wave function based approach that relies on the mean-field approximation. It is the basis of molecular orbital (MO) theory, which hypothesizes that each electron's motion can be described by a single-particle function (orbital) which does not depend explicitly on the instantaneous motions of the other electrons. HF theory often provides a good starting point for more elaborate theoretical methods which are better approximations to the electronic Schrodinger equation and is also referred to as an independent particle model or a mean field theory.

The HF equations form a self-consistent problem in the sense that the wave functions determine the mean field, while the mean field in turn determines the wave functions. In practice this leads to iterative solutions in which one starts from an initial guess for the wave functions for spin-Orbitals, such as harmonic-oscillator states and determines the mean field from them. Solving the Schrödinger equations



yields a new set of wave functions, and this process is repeated until, convergence is achieved. This method of solution is often called self-consistent field method.

The HF method assumes that the exact,  $N$ -body wave function of the system can be approximated by a single Slater determinant (in the case where the particles are fermions) or by a single permanent (in the case of bosons) of  $N$  spin-orbitals. HF wave function is written as a Slater determinant that ensures the electrons are indistinguishable and are therefore associated with every orbital. Slater determinant is an expression that describes the wave function of a multi-fermionic system that satisfies anti-symmetry ( $\Phi = 0$ ) requirements and subsequently the Pauli Exclusion Principle by changing sign upon exchange of fermions. The Slater determinant arises from the consideration of a wave function for a collection of electrons, each with a wave function known as the spin-orbital,  $\chi(\mathbf{x})$ , where  $\mathbf{x}$  denotes the position and spin of the singular electron. By invoking the variational principle, one can derive a set of  $N$ -coupled equations for the  $N$  spin orbitals. Solution of these equations yields the HF wave function and energy of the system, which are approximations of the exact ones. The solutions to the resulting non-linear equations behave as if each particle is subjected to the mean field created by all other particles. The equations are almost universally solved by means of an iterative, fixed-point type algorithm.

When the molecular ground-state is not a singlet state, or in situations where chemical bonds are stretched, i.e. in dissociation process, a restricted closed shell HF determinant is not able to describe, even qualitatively, the electronic distribution. There are two possible ways of applying the HF theory [42].

In the approach, termed Restricted Open-Shell HF, spin-adapted configuration state functions (CSFs) are used, i.e. linear combinations of Slater determinants, but in such a case the HF equations are rather more complicated. In a simpler approach, called Unrestricted Hartree-Fock, UHF, electrons with  $\alpha$  and  $\beta$  spins are described by different spatial function. Two sets of HF equations must be solved in the SCF procedure, one set for the set of spatial orbitals with  $\alpha$  spin, and one set for the set of spatial orbitals with  $\beta$  spin.

## 2.2 Density Functional Theory

Density functional theory (DFT) [42] is an extremely successful approach for the description of ground state properties of metals, semiconductors, and insulators. For determination of structures (corresponding to energy minima) it is generally surprisingly accurate, giving inter atomic distances with a typical accuracy of (+0.02) Å. The main idea of DFT is to describe an interacting system via its density and not via its many-body wave function. The electron density is a fundamental quantity in quantum chemistry that gives the probability of finding an electron in the volume element. It is a function of three variables (x, y and z) and is therefore relatively easy to visualise. DFT focuses on functional that return the energy of the system [42].

A functional is defined as a function of a function, and the energy of the molecule is a functional of the electron density. The electron density is a function with three variables x, y, and z position of the electrons. Unlike the wave function, this becomes significantly more complicated as the number of electrons increases; the determination of the electron density is independent of the number of electrons. There are roughly three types, or categories, of density functional methods.

- *Local density approximation (LDA)* methods assume that the density of the molecule is uniform throughout the molecule, and is typically not a very popular or useful method.
- *Gradient-corrected (GC)* methods look to account for the non-uniformity of the electron density.
- *Hybrid* methods, as the name suggests, attempt to incorporate some of the more useful features from *ab initio* methods (specifically Hartree-Fock methods) with some of the improvements of DFT mathematics.

### **2.3 Tools Used in the Study**

In our study on Ni-Mn-Ga, both HF and DFT methods are being used and analysis is done with Gaussian 03W [43] software package. In addition to Gaussian, few other tools are also used. Powder cell [44] is used for arriving at the Cartesian atomic coordinates to provide input to Gaussian. Gauss View [45], Gauss sum [46], Chemcraft [47] and Gabedit [48] are the other packages used for analysing and interpreting the Gaussian output. Brief introduction about the software packages are given below.

### 2.3.1 Powder Cell

Powder Cell is an excellent tool [44] for the structure determination using powder diffraction data. It supports the structure determination in a relatively short time by the use of crystallographic and crystal chemical knowledge. Powder Cell for Windows is a GUI based program for exploring, manipulating crystal structures and calculating powder patterns. It provides extended overview of all generated atomic positions, bonding angles and distances, space-group information that includes general and special positions, Wyckoff notation and list of all maximal subgroups. Also the user shall be able to manipulate in an easy way (translation and rotation of atoms or molecules; change, delete and insert atoms or molecules, symmetry reduction etc.).

### 2.3.2 Gaussian 03W

Gaussian [43] is a computational chemistry software program initially released in 1970 by theoretical chemist, Nobel-Prize laureate John Pople and his research group at Carnegie-Mellon University as Gaussian 70. It has been continuously updated since then. The name originates from Pople's use of Gaussian orbitals to speed up calculations compared to those using Slater-type orbitals, a choice made to improve performance on the limited computing capacities of earlier hardware for HF calculations. The software runs on virtually all computer platforms, including Microsoft Windows, Macintosh OS, and all variants of UNIX. Gaussian is capable of running all of the major methods in molecular modeling, including molecular mechanics, ab initio, semi-empirical, and DFT. It is probably best known for its robustness in running ab initio and DFT calculations.

Running Gaussian involves the following activities:

- Creating Gaussian input describing the desired calculation.
- Specifying the locations of the various scratch files.
- Specifying resource requirements.
- Initiating program execution

Gaussian uses several scratch files in the course of its computation. The very useful one is the Checkpoint file and Formatted check point file. Gaussian 03 inputs consist of a series of lines in an ASCII text file.

The basic structure of a Gaussian input file includes several different sections:

- Link 0 Commands: Location and name of scratch files.
- Route section (# lines): Specification of desired calculation type, model chemistry and other options.
- Title section: Brief description of the calculation.
- Molecule specification: Specification of molecular system to be studied.

Text based Gaussian input file whose extension is .gjf is described below.

%chk=frq.chk		Link 0 section
%nproc=15		
#B3LYP/6-31G** SCF= (Int Rep, QC) freq		Route section
Frequency calculations for Austenite		Title section
0 1		Molecular specification
Ga	0.0000 0.0000 0.0000	
Ni	1.4528 1.4528 1.4527	
Mn	2.9055 0.0000 0.0000	
Mn	0.0000 2.9055 0.0000	
Ga	2.9055 2.9055 0.0000	
Mn	0.0000 0.0000 2.9055	
Ga	2.9055 0.0000 2.9055	
Ga	0.0000 2.9055 2.9055	
Mn	2.9055 2.9055 2.9055	

The route section of a Gaussian 03 input file specifies the type of calculation to be performed. There are three key components to this specification:

- The job type
- The method
- The basis set

The combination of method and basis set specifies model chemistry to Gaussian, specifying the level of theory. Every Gaussian job must specify both a method and a basis set. This is usually accomplished via two separate keywords within the route section of the input file, although a few method keywords imply the choice of basis set.

### **2.3.3 Gauss View**

Gauss View [45] is an affordable, full-featured graphical user interface for Gaussian. Gauss View supports all Gaussian features, and it includes graphical facilities for analysing the results of the calculations via state-of-the-art visualization features. Currently, it stands as a part of the Gaussian Package. By subscribing to Gaussian, direct access to run Gauss View is possible.

### **2.3.4 Gauss Sum**

Gauss Sum [46] is a GUI application that can analyse the output of ADF, GAMESS (US), GAMESS-UK, Gaussian, Jaguar and PC GAMESS to extract and calculate useful information. This includes the progress of the SCF cycles, geometry optimisation, UV-Vis/IR/Raman spectra, MO levels, MO contributions and more.

### **2.3.5 Gabedit**

Gabedit [48] is a graphical user interface to computational chemistry packages like Gamess-US, Gaussian, Molcas, Molpro, MPQC, Open Mopac, Orca, PC Gamess and Q-Chem developed by Abdul-RahmanAllouche.

### **2.3.6 Chemcraft**

Chemcraft [47] is a graphical program for working with quantum chemistry computations. It is a convenient tool for visualization of computed results and preparing new jobs for the calculation. Chemcraft is mainly developed as a graphical user interface for Gamess and Gaussian program packages. For working with other formats of calculations, the possibility to import/export coordinates of atoms in text format can be easily used. Chemcraft does not perform its own calculations, but can

significantly facilitate the use of widespread quantum chemistry packages. Chemcraft works under Windows and Linux.

The main capabilities of the program include:

- Rendering 3-dimensional pictures of molecules by atomic coordinates with the possibility to examine or modify any geometrical parameter in the molecule (distance, angle etc.).
- Visualization of Gamess, Gaussian, NWChem, ADF, Molpro, Dalton, Jaguar, Orca, Q Chem output files: representation of individual geometries from the file (optimized structure, geometry at each optimization step, etc.), animation of vibrational modes, graphical representation of gradient (forces on nucleus), visualization of molecular orbitals in the form of ISO surfaces or colored planes, visualization of vibrational or electronic spectra, possibility to show SCF convergence graph.

## Chapter 3

### Electronic and Structural Properties of Austenite Ni-Mn-Ga

#### 3.1 Structure Generation through Powder Cell

For performing Gaussian analysis *Molecular specification* of the system must be specified in the Gaussian input. This was a major challenge in the study of Ni-Mn-Ga since such data was not available due to the complexity of the system. Using JCPDS data numbered 65-0618 that depicts Ni-Mn-Ga as a face centred cubic lattice with space group no: 225 and lattice constant  $5.823 \text{ \AA}$ , structure is generated using Powder cell and the x, y, z Cartesian coordinates of the unit cell are found. Gaussian jobs are submitted by sending a text-based input file to the Gaussian processor, and the results are returned as text-based output files.

The different lattice constants used by various researchers are chosen for the study, total DFT energy is calculated as a function of the lattice parameter, to optimize the  $L2_1$  structure of ferromagnetic Ni-Mn-Ga Heusler alloy.

The present study shows the equilibrium lattice constant of austenite Ni-Mn-Ga is having the value  $5.811 \text{ \AA}$  ( $10.981 \text{ a.u.}$ ). This is in good agreement with results from neutron and x-ray diffraction measurements and previous theoretical studies [4]. Ayuela et al [13] has found the theoretical lattice constant using FLAPW method to be  $5.81 \text{ \AA}$  ( $10.981 \text{ a.u.}$ ) which is perfectly identical to the current finding. The experimental value arrived by them was  $11.01 \text{ a.u.}$

Ozdemir Kart et al , carried out spin-polarized total energy calculations by using the Vienna ab initio simulation package (VASP) and the implemented projector augmented wave pseudopotential formalism (PAW) and reported  $a=5.812 \text{ \AA}$  [33]. For the cubic austenitic phase, Barman et al, [49] calculated the equilibrium lattice constant to be  $10.998 \text{ a.u.}$  ( $5.820 \text{ \AA}$ ) and they have reported  $11.004 \text{ a.u.}$  from their x-ray diffraction measurements.

#### 3.2. Vibrational Analysis

Infrared radiation is absorbed by molecules and converted into energy of molecular vibration. In IR spectroscopy, the molecule is exposed to infrared radiation. [50, 51] When the radiant energy matches the energy of a specific molecular vibration, absorption occurs. IR study for organic molecules are reported extensively in literature. Inorganic analysis is less researched since their vibrational spectra are too weak, more difficult to obtain and do not appear in common middle infrared region ( $4000 - 400 \text{ cm}^{-1}$ ) but emerge in far infrared region (under  $400 \text{ cm}^{-1}$ ).

The vibrational frequency calculations for Ni-Mn-Ga at B3LYP and HF levels using the 6-31G\*\* basis set were done in the study. The 'freq' keyword enables the required study. Since the system under study is very large one and poses serious convergence error, SCF=QC is given in the Route section for successful Gaussian run. Gabedit and Chemcraft program were used in the analysis of the output. The visualisation tool Chemcraft allows viewing the vibrations of the atoms for each vibration mode with the displacement vector in its image window. Assignments were made through visualization of the atomic displacement representations for each vibration, viewed through Chemcraft 1.6 and frequency range in the spectrum of our result matches with similar study of Alexey T. Zayak [52].

### **3.3 Thermo Chemistry**

The results of thermo chemical calculations reveal in the case of entropy translational, vibrational and rotational modes all have significant contributions but the thermal energy arises mainly from vibrational modes.

### **3.4 Visualization of Molecular Orbitals**

The starting point for understanding molecular properties is the atom. Atoms have two important aspects: the number of electrons and the spatial distribution of these electrons. The HOMO is the Molecular Orbital of Highest Energy that is occupied by electrons. The LUMO is the Molecular Orbital of Lowest Energy that is not occupied by electrons. HOMO represents the ability to donate an electron and LUMO represents the ability to accept an electron. The HOMO, LUMO energies of Ni-Mn-Ga have been calculated at B3LYP/6-31G \*\* method and the energy gap presented reflects the chemical activity of the molecule. Among the six subsequent



excited states calculated, the strongest transitions appear between HOMO to LUMO orbitals. The numerical value of energy gap between HOMO-LUMO orbitals calculated at B3LYP level is -0.045740209 a.u. Distribution of atomic charges is also viewed from the density calculations. The result of our isosurface study of electron density of the unit cell matches with findings reported by Breczko et al [35].

### 3.5 Nuclear Magnetic Resonance

Nuclear magnetic resonance (NMR) is a physical phenomenon in which magnetic nuclei in a magnetic field absorb and re-emit electromagnetic radiation. This energy is at a specific resonance frequency which depends on the strength of the magnetic field and the magnetic properties of the isotope of the atoms. NMR allows the observation of specific quantum mechanical magnetic properties of the atomic nucleus.

The Gaussian output for the austenite phase of Ni-Mn-Ga with the NMR=spin keyword resulted in the spectrum. Nickel has very low relative sensitivity (0.00357) and very low abundance (1.19%) and so it doesn't show its contribution in the NMR spectrum. Natural abundance of Gallium-71 and Manganese-55 are 39.6% and 100% respectively. The relative sensitivity of Gallium is 0.14 and of Manganese is 0.18 which are really high and they show their role in the NMR spectrum [53].

Mn <sup>55</sup> has  $I = 5/2$  and because the electron distribution around the nucleus is not uniform it results in Electric Field Gradient (EFG). Due to this EFG nuclear energy level undergo splitting into three levels namely  $\pm 1/2$ ,  $\pm 3/2$  and  $\pm 5/2$ . Due to unpaired electrons around the nucleus, a feeble magnetic field is produced and this causes dipole interaction that result in  $\pm 1/2$  level to split into  $+1/2$  and  $-1/2$  levels. Four levels  $+1/2$ ,  $-1/2$ ,  $\pm 3/2$  and  $\pm 5/2$  are finally formed. Transitions that obey the Lapoite's selection rule namely  $\Delta m_I = \pm 1$  only are allowed. Therefore for  $I = 5/2$ , transitions from  $+1/2$  to  $-1/2$ ,  $-1/2$  to  $-3/2$  and  $\pm 3/2$  to  $\pm 5/2$  are possible which results in the triplet as achieved in our output.

In the same way Ga has  $I = 3/2$ . Due to EFG two levels  $\pm 1/2$  and  $\pm 3/2$  are formed. Feeble magnetic field due to unpaired electrons results in  $\pm 1/2$  level to split into  $+1/2$  and  $-1/2$  levels and finally three levels  $+1/2$ ,  $-1/2$  and  $\pm 3/2$  are resulted. The

possible transitions obeying the selection rules are  $+1/2$  to  $-1/2$  and  $-1/2$  to  $-3/2$  and they result in a doublet as obtained in the NMR spectrum.

The change in the effective field on the nuclear spin causes the NMR signal frequency to shift. The magnitude of the shift depends upon the type of nucleus and the details of the electron motion in the nearby atoms and molecules. It is called a "chemical shift".

### **3.6 DOS Spectrum using Gauss Sum**

The density of states (DOS) of a system describes the number of states per interval of energy at each energy level that are available to be occupied by electrons. The density distributions are not discrete like a spectral density but continuous. A high DOS at a specific energy level means that there are many states available for occupation. A DOS of zero means that no states can be occupied at that energy level. Molecular orbital information is extracted from the Gaussian output whose input had the keyword density. The density of states diagram is convoluted from the molecular orbital data.

## Chapter 4

### Electronic and Structural Properties of Orthorhombic and Tetragonal Martensite Ni-Mn-Ga

#### 4.1.1 Generating Martensite Orthorhombic Structure

The martensitic transformation of Ni-Mn-Ga and the structure of this phase were studied by powder X-ray diffraction experiment by Lara et al [54]. The symmetry of the basic structure was found to be orthorhombic. The structure is refined by Rietveld method with super space group *Immm* having 'a' = 4.2187 Å, 'b' = 5.5534 Å and 'c' = 4.1899 Å. Using these lattice parameters and the space group as the input to Powder cell, the Cartesian coordinates were generated for the current study.

#### 4.1.2 Vibrational Analysis

Vibrational spectroscopy is the study of the interaction of radiation with molecular vibrations but differs in the manner in which photon energy is transferred to the molecule by changing its vibrational state. IR spectroscopy measures transitions between molecular vibrational energy levels as a result of the absorption of IR radiation.

Vibrational study of martensite Orthorhombic Ni-Mn-Ga for Density functional and Hartree-Fock methods are carried out using Gaussian with freq keyword. Detailed descriptions of the nature of vibrations are analysed and assignments were made through visualization of the atomic displacement representations for each vibration, viewed through Chemcraft 1.6.

#### 4.1.3 Thermo Chemistry

The results of thermo chemical calculations are reported. All computed results are at 298.15K and at 1 atm. pressure. For the case of entropy translational, vibrational and rotational modes all have significant contributions. Also it was found the thermal energy arises mainly from vibrational modes.

#### 4.1.4 Visualization of Molecular Orbitals

The HOMO, LUMO energies of Martensite orthorhombic Ni-Mn-Ga have been calculated at B3LYP/6-31G\*\* method. The energy gap obtained reflects the chemical activity of the molecule. Among the subsequent excited states calculated, the strongest transitions appear between HOMO to LUMO orbitals. The numerical value of energy gap between HOMO-LUMO orbitals calculated at B3LYP level is - 0.04809a.u.

#### 4.1.5 Nuclear Magnetic Resonance

The same reasoning for NMR spectra of Austenite holds for Martensite structure also since the result showed the same spectrum. Nickel has very low relative sensitivity (0.00357) and very low abundance (1.19%) and so it doesn't show its contribution in the NMR spectrum. Natural abundance of Gallium-71 and Manganese-55 are 39.6% and 100% respectively. The relative sensitivity of Gallium is 0.14 and of Manganese is 0.18 which are really high and they show their role in the NMR spectrum.

### 4.2 The Study of Martensite Tetragonal Structure

A new model for the tetragonal Ni-Mn-Ga was developed by Wedel et al., [30] with the help of TEM data, X-ray powder diffraction measurements, and a computational simulation based on the X-ray powder diffraction patterns and they confirmed the tetragonal symmetry with the lattice parameters  $a=3.88 \text{ \AA}$ ,  $c=6.48 \text{ \AA}$ ; space group:  $I_4/mmm$ ; Using these lattice parameters and the space group as the input to Powder cell, the Cartesian coordinates are generated and used in the Gaussian analysis.

#### 4.2.1. Vibrational Analysis of Tetragonal Structure

Vibrational study of martensite tetragonal Ni-Mn-Ga for Density functional and Hartree-Fock methods are carried out using Gaussian with freq keyword. Detailed descriptions of the nature of vibrations are analysed and assignments are made through visualization of the atomic displacement representations for each vibration, viewed through Chemcraft1.6.

#### **4.2.2. Thermo Chemistry**

The results of thermo chemical calculations are reported. All computed results are at 298.15K and at 1 atm. pressure. For the case of entropy translational, vibrational and rotational modes all have significant contributions. Also it was found the thermal energy arises mainly from vibrational modes.

#### **4.2.3. Visualization of Molecular Orbitals**

The HOMO, LUMO energies of Martensite tetragonal Ni-Mn-Ga have been calculated at B3LYP/6-31G\*\* method. The energy gap obtained reflects the chemical activity of the molecule. Among the subsequent excited states calculated, the strongest transitions appear between HOMO to LUMO orbitals. The numerical value of energy gap between HOMO-LUMO orbitals calculated at B3LYP level is -0.05374a.u.

#### **4.2.4. Nuclear Magnetic Resonance**

The same reasoning for NMR spectra of Austenite holds for Martensite structure also since the result showed the same spectrum. Nickel has very low relative sensitivity (0.00357) and very low abundance (1.19%) and so it doesn't show its contribution in the NMR spectrum. Natural abundance of Gallium-71 and Manganese-55 are 39.6% and 100% respectively. The relative sensitivity of Gallium is 0.14 and of Manganese is 0.18 which are really high and they show their role in the NMR spectrum.

#### **4.2.5. DOS Spectrum of both the Structures of Martensite Phase using Gauss Sum**

The density of states diagram is convoluted from the molecular orbital data. It is evident from the DOS spectrum of the austenite phase and that of martensite that the majority densities of states for both cubic and martensite are essentially identical. The peak just below the Fermi energy broadens in the orthorhombic martensite, transferring spectral weight out of occupied Ni d-states. Interaction of d-states is indicated in the phase transformation.

## **Chapter 5**

### **Magneto-Mechanical Properties of Polycrystalline Ni-Mn-Ga Ferromagnetic Shape Memory Alloys**

#### **5.1. Introduction**

Four different polycrystalline Ni-Mn-Ga alloys were prepared by substituting Mn on Ni, Ga and both (Ni, Ga site) and the study of effect of Mn substitution on structural, magnetic and transformation behavior of Ni-Mn-Ga alloy was performed. It was found that the substitution of Mn on Ni site decreases the transformation temperatures and the substitution of Mn on Ga site increases the transformation temperatures. Lattice distortion of Mn site on Ni and Ga sites changes the crystal structure from cubic to tetragonal and orthorhombic. Microscopic studies confirm the presence of twins in the material. Magnetic studies reveal that the addition of Mn atom stabilizes the Ni atom which increases the ferromagnetic ordering of the alloy. Compression studies reveal that magnetic and mechanical training increases the field induced strain in the alloy. The training effect on the mechanical behavior of the alloy has been performed to study the actuation behavior of the alloy.

#### **5.2. Experimental Procedure**

Ni-Mn-Ga FSMAs are prepared using arc melt furnace. The starting materials Nickel, Manganese and Gallium (liquid) are taken in the form of powders with a purity of 99.999% and melted using tungsten electrode. The sample is reverted and remelted four times to ensure the uniform chemical dispersion and alloying. Then the sample is annealed in a vacuum furnace at 1073 K to ensure the homogeneity of the alloy. Four different alloys are prepared and the compositions are Ni<sub>50</sub>-Mn<sub>25</sub>-Ga<sub>25</sub>, Ni<sub>48</sub>-Mn<sub>26</sub>-Ga<sub>26</sub>, Ni<sub>52</sub>-Mn<sub>28</sub>-Ga<sub>20</sub> and Ni<sub>49</sub>-Mn<sub>30</sub>-Ga<sub>21</sub>. The crystal structures of the alloys at room temperature are studied by X-Ray Diffractometer. The forward and reverse martensite transformations are determined using Differential Scanning Calorimetry in the range from 123 K to 423 K with a scanning rate of 5 K / min. The exchange coupling interaction of the alloy is studied through magnetic measurements. The alloy is magnetically trained to remember its parent phase. Further it is

mechanically trained under compressive load by using Universal Testing Machine (UTM). The pseudo elastic behavior of the alloy has been analyzed using UTM.

### **5.3. Results and Discussion**

#### **5.3.1 Diffraction Studies on Ni-Mn-Ga Alloy**

The characteristic reflections of the XRD patterns are indexed by comparing the patterns with the reported JCPDS data. The structure of the off stoichiometric  $\text{Ni}_{50}\text{Mn}_{25}\text{Ga}_{25}$  was found to be  $L2_1$  cubic structure. A slight increase in Mn content distorts lattice sites as a result structural transition occurs from  $L2_1$  cubic to B2 phase which belongs to martensite phase. Tetragonal martensite is observed when the composition of the manganese is increased to 28%. Further increase in Mn composition changes tetragonal structure to orthorhombic where the MFIS is high which shows that the twin boundary movement is high in this alloy. The size factor is responsible for the lattice distortions. The atomic radius of Ni, Mn and Ga are 0.125, 0.127 and 0.141 nm. A slight increase in cell volume is observed when Mn atom substitutes Ni atom. A large fall in the unit cell volume is obtained when Mn atom replaces Ga atom. The results found in this study well agree with Jiang et al work [55].

#### **5.3.2. Transformation Behavior of Ni-Mn-Ga Alloy**

Exothermic peak observed in the DSC cooling curve is due to the thermo-elastic martensitic transformation and correspondingly an endothermic peak observed in the heating curve is due to the austenitic transformation. It is observed that the antiferromagnetic ordering dominates when Mn content reaches 30% which is evident by the drop observed in the curie transition and transformation temperatures. The transformation temperatures were increased when Mn replaces Ga atom and it decreases when Mn atom replaces Ni atom. The transformation temperature increases with increase of Mn concentration and Mn/Ga ratio. The drop in the curve near 30% is because of Mn replacing Ni. The Curie temperature is not affected much with the composition changes. Kokorin et al reported that the decrease in unit volume increases the transformation temperatures of the alloy [14]. The results obtained in the study well agree with Jiang et al work [55].

### **5.3.3. Microstructural Behavior of Ni-Mn-Ga Alloy**

SEM studies have been done to detect the presence of twins in the alloy and it is indicated by a line. Micro cracks are observed in the image and depending on the crack propagation in the alloy; and enabled defining the toughness of the alloy. In transgranular fracture, the crack initiated inside the grain and then propagates from one grain to another grain. It strengthens the grain boundary of the alloy and thereby increases the fracture toughness. It is inferred that the fracture present in the alloy is transgranular and as a result, the material has high fracture toughness. The results match with Wang et al work [56]. Increase in toughness shows that the ductility of the alloy is increased.

### **5.3.4. Magnetic Behaviour of Ni-Mn-Ga Alloy**

The effect of Mn concentration on the magnetic behavior of the alloy was studied and it is observed that the magnetic moment of the alloy decreases with increase in e/a. It shows that antiferromagnetic exchange interaction dominates when the free electron concentration increases. The decrease in magnetic moment when Mn replaces Ga atom induces the antiferromagnetic coupling exchange interaction in the alloy. The position of atom plays a vital role in determining the exchange coupling interaction in the alloy.

### **5.3.5. Stress-Strain Behaviour of Ni-Mn-Ga Alloy**

The stress versus strain curve for the  $\text{Ni}_{50}\text{Mn}_{25}\text{Ga}_{25}$  is traced by training the samples in a constant magnetic field for hours together. A 2% strain has been and it is higher than the reported values. Twin boundary motion is responsible for flattening in the curves. The idealized curve contains two plateaus. The upper plateau in the loading curve is because of the transformation from austenite to martensite and detwinning occurs in the newly formed martensite. The lower plateau represents the stress strain behavior of the ferromagnetic shape memory alloy during unloading process where the martensite transforming in to austenite. This confirms the superelastic behavior of the FSMAs. It is noted that there is no permanent deformation upon unloading; part of mechanical energy used to deform the alloy is



lost during unloading. Before training, the material doesn't show the mechanical hysteresis. Mechanical training is performed to get the mechanical hysteresis curve. The mechanical training changes the twin structures i.e. the coarsening of twins and therefore increases in internal stress which was reported by Gaitzsch [57]. After twelfth cycle, the mechanical hysteresis is observed. The strain observed is varied from 1.5 % to 2 %. The strain observed is higher than the reported one [57].

#### **5.4. Conclusion**

Mn atom is systematically substituted in Ni-Mn-Ga and the effect on structural, transformation, magnetic and mechanical behavior of the alloy has been studied. Structural studies confirm that the substitution of Mn in Ni, Ga and in both sites induces the lattice distortion which changes the crystal structure from cubic structure to orthorhombic structure. The field induced strain is high in the orthorhombic crystal. The transformation temperature increase when Mn replaces Ga but it is reverse when Mn replaces Ni. The substitution of Mn on Ni site decreases the transformation temperature and if it replaces Ga where transformation temperatures increase. Mechanical studies reveal that about 2% strain is achieved in Ni-Mn-Ga alloy. Stress wave propagation studies reveal that the stress amplitude of the alloy increases with the increase of  $e/a$ . It is concluded from the high transformation temperatures, exchange interaction and the high stress amplitude that this material can be used as actuators in the magnetic actuation applications.

## **Chapter 6**

### **Results and Discussion**

Our study on FSMA Ni-Mn-Ga is of two parts, theoretical analysis using Gaussian 03W to predict electronic and structural properties and experimental procedures to find magneto-mechanical properties of polycrystalline Ni-Mn-Ga. Both Hartree–Fock and Density functional theory are being used in theoretical analysis. To provide input to Gaussian, the tool Powder cell is used. For investigating the Gaussian output, other packages namely Gauss View, Gauss sum, Chemcraft and Gabedit are used. Though it is a first attempt, the study demonstrates HF and DFT calculations using Gaussian offer a powerful approach in analysing the alloy Ni-Mn-Ga.

The study shows the equilibrium lattice constant of Ni-Mn-Ga Heusler alloy equal to 5.811 Å, which is in a good agreement with other theoretical and experimental findings. IR Spectral studies, detailed assignment and descriptions of the nature of vibrations in Ni-Mn-Ga help reasoning the peaks in the IR Spectra. The frequency range of the present study matches with literature as mentioned in chapters 3 and 4. Similarly NMR spectra allow us to better understand chemical environment of the specific nuclei that results in shielding or de-shielding. Spin spin calculations also provide better insight into the nuclear energy levels.

Molecular orbital visualization and calculated energy gap enable us to understand the system well. The DOS spectrum for austenite phase and both the martensite orthorhombic and tetragonal phases were convoluted from molecular orbital data and the DOS spectrum for both cubic and martensite are essentially identical and there are only limited changes. The peak just below the Fermi energy broadens in the orthorhombic martensite, indicating interaction in d states.

Study of magnetic properties using Gaussian 03W is in progress. Gaussian poses lot of challenges like need of cluster computing and requisite of specialized mechanism to deduce the Z matrix to be fed as input. Researcher also must be ready to explore ways to avoid convergence errors and to endure with long computing hours claimed by Gaussian.

Hence experimental study of Ni-Mn-Ga was done to supplement the theoretical work. Structural studies confirm that the substitution of Mn in Ni, Ga and in both sites induces the lattice distortion which changes the crystal structure from cubic to orthorhombic. The field induced strain is high in the orthorhombic crystal. The transformation temperature increase when Mn replaces Ga but it is reverse when Mn replaces Ni. The substitution of Mn on Ni site decreases the transformation temperature and if it replaces Ga transformation temperatures increase. Mechanical studies reveal that about 2 % strain is achieved in Ni-Mn-Ga alloy. Stress wave propagation studies reveal that the stress amplitude of the alloy increases with the increase of  $e/a$ .

This study is unique in the sense it has used Gaussian 03W offer a potent approach in analysing the alloy Ni-Mn-Ga. It opens the future valuable research of using Gaussian for large systems also. There is a good scope for further analysis of the same system with higher version of Gaussian namely 09W, which is expected to be faster and additional study feasible through new functionalities introduced in the higher version.

## References

- [1] O'Handley R C, Allen S M, Shape memory alloys, magnetically activated ferromagnetic shape memory materials, Schwartz M (ed.), Encyclopaedia of Smart Materials. John Wiley and Sons, New York, 936-951 (2001).
- [2] O'Handley R C, Modern Magnetic Materials, John Wiley & Sons Inc., New York, (2000).
- [3] Ullakko K, Huang J K, Kantner C, and O'Handley R C, Large magnetic-field induced strains in Ni<sub>2</sub>MnGa single crystals, Applied Physics Letters, **69**, 1966-68 (1996).
- [4] Ullakko K, Huang J K, Kokorin V V and O'Handley R C, Magnetically controlled shape memory effect in Ni<sub>2</sub>MnGa inter metallics, ScriptaMaterialia, **36, No. 10**, 1133-1138 (1997).
- [5] O'Handley R C, Model for strain and magnetization in magnetic shape memory alloys, Journal of Applied Physics, **83**, 3263-3270 (1998).
- [6] Murray S J, Marioni M A, Allen S M, O'Handley R C, Lograsso T A, 6% magnetic-field-induced strain by twin-boundary motion in ferromagnetic Ni-Mn-Ga, Applied Physics Letters, **77**, 886-889 (2000).
- [7] Paul D I, O'Handley R C, Peterson B, Ferromagnetic shape memory alloys: Theory of interactions, Journal of Applied Physics, **97**, 10M312-10M312-3 (2005).
- [8] Paul D I, McGehee, O'Handley R C, Richard M, Ferromagnetic shape memory alloys: A theoretical approach, Journal of Applied Physics, **101**, 123917(1)-123917(9) (2007).
- [9] Marioni M A, O'Handley R C, Allen S M, Hall S R, Paul D I, Richard M L, Feuchtwanger J, Peterson B W, Chambers J M, Techapiesancharoenki R, The

- ferromagnetic shape-memory effect in Ni–Mn–Ga, *Journal of Magnetism and Magnetic Materials*, **290-291**, Part 1, 35-41 (2005).
- [10] O’Handley R C, Paul D I, Allen S M, Richard M, Feuchtwanger J, Peterson B, Techapiesancharoenkij R, Barandiaran M, Lazpita P, Model for temperature dependence of field-induced strain in ferromagnetic shape memory alloys, *Materials Science and Engineering A***438**, 445–449 (2006).
- [11] Kainuma R, Nakano H, and Ishida K, Martensitic transformations in NiMnAl  $\beta$  phase alloys, *Metallurgical and Materials Transactions, A*, **27**, 4153-4162 (1996).
- [12] Cong D Y, Wang S, Wang Y D, Ren Y, Zuo L, and Esling C, Martensitic and magnetic transformation in Ni-Mn-Ga-Co ferromagnetic shape memory alloys, *Materials Science and Engineering A*, **473**, 213-218 (2008).
- [13] Ayuela A, J Enkovaara, K Ullakko and R Nieminen, Structural properties of magnetic Heusler alloys. *Journal of Physics: Condensed Matter*, **11**, 2017-2026 (1999).
- [14] Martynov V, and V Kokorin, The crystal structure of thermally and stress induced martensites in Ni<sub>2</sub>MnGa single crystals, *Journal of Physics III (France)* **2**, 739-749 (1992).
- [15] Ullakko K, A Sozinov and P Yakovenko, Large magnetic field induced strains in Ni-Mn-Ga alloys due to redistribution of martensitic variants, *Condensed Matter*, 0004211-4 (2000).
- [16] Barandiarán J M, Chernenko V A, Lázpita P, Gutiérrez J, and Feuchtwanger J, Effect of martensitic transformation and magnetic field on transport properties of Ni-Mn-Ga and Ni-Fe-Ga Heusler alloys, *Physical Review B*, **80**, 104404-11 (2009).
- [17] Murray S J, Marioni M, Tello P G, Allen S M, O’Handley R C, Giant magnetic-field-induced strain in Ni-Mn-Ga crystals: Experimental results and modeling. *Journal of Magnetism and Magnetic Materials*, **226–230**, 945–947 (2001).

- [18] Sozinov A, Likhachev AA, Lanska N, Ullakko K, Giant magnetic-field-induced strain in NiMnGa seven-layered martensitic phase, Applied Physics Letters, **80**, 1746-1748 (2002).
- [19] Chernenko V A, Chmielus M, and Müllner P, Large magnetic-field-induced strains in Ni-Mn-Ga nonmodulated martensite, Applied Physics Letters, **95**, 104103 (1) – 104103 (3) (2009).
- [20] Dunand D, Zhang Z, Mullner P, Chmielus M, and Witherspoon C, Giant Magnetic-Field-Induced Strains in Polycrystalline Ni-Mn-Ga Foams, Nature Materials Journal, **8**, No.11, 863-866 (2009).
- [21] Heczko O, Sozinov A, and Ullakko K, Giant field induced strain by twin boundary motion in ferromagnetic Ni-Mn-Ga, IEEE Transactions on Magnetics, **36**, 3266-3268 (2000).
- [22] Heczko O, Sozinov A, and Ullakko K, Giant field- induced reversible strain in magnetic shape memory NiMnGa alloy, IEEE Transactions on Magnetics, **38**, 2814-2816 (2002).
- [23] O'Handley R C, Murray S J, Marioni M, Nembach H, and Allen S M, Phenomenology of Giant Magnetic-Field induced Strain in Ferromagnetic Shape Memory Materials, Journal of Applied Physics , **87**, 4712-4717 (2000 b).
- [24] Chernenko V A, L'vov, Pons J, Cesari E, Rudenkob A A, Dated H, Matsumotod M, Kanomatad T, Stress-strain behaviour of Ni-Mn-Ga alloys: experiment and modelling, Materials Science and Engineering A, **378**, 349-352 (2004).
- [25] Singh R K and Gopalan R, Martensite transformation and magnetic property dependence on the annealing temperature in Ni-rich Ni-Mn-Ga alloy, Advanced Materials Research, **52**, 57-62 (2008).

- [26] Singh R K, Shamsuddin M, Gopalan R, Mathur R P, Chandrasekaran V, Magnetic and structural transformation in off-stoichiometric NiMnGa alloys, *Materials Science and Engineering A*, **476**, 195–200 (2008).
- [27] VallalPeruman K, Mahendran M and Seenithurai S, Magnetic properties of single crystalline Ni-Mn-Ga ferromagnetic shape memory alloy, *Physica B* **355**, 172-175 (2009).
- [28] ManickamMahendran, Micro structural analysis and phase transformation in Ni – Mn – Ga ferromagnetic shape memory alloys, *Smart Materials and Structures*, **14**, 1403–1409 (2005).
- [29] Awaji, Watanabe K, Matsumoto M and Kobayashi N, Investigation of phase transformations in Ni<sub>2</sub>MnGa using high magnetic field low-temperature X-ray diffraction system, *Physica B*, **284**, 1333-1334 (2000).
- [30] Wedel B, Suzuki M, Murakami Y, Wedel C, Suzuki T, Shindo D, Itagaki K, Low temperature crystal structure of Ni-Mn-Ga alloys. *Journal of Alloys and Compounds*, **290**, 137–143 (1999).
- [31] Barandiaran J M, Chernenko V A, Lazpita P, Gutierrez J, Orue I, Feuchtwanger J, and Besseghini S, Magnetic field effect on premartensitic transition in Ni-Mn-Ga alloys, *Applied Physics Letters*, **94**, 051909–051912 (2009b).
- [32] Barandiarán J M, Jon Gutiérrez, Patricia Lázpita, J Feuchtwanger, Neutron Diffraction Studies of Magnetic Shape Memory Alloys ,*Materials Science Forum*, **684**, 177-201 (2011).
- [33] Ozdemir Kart S, Uludogan M, Karaman I, Cagin T, DFT studies on structure, mechanics and phase behavior of magnetic shape memory alloys: Ni<sub>2</sub>MnGa, *Physica Status Solidi*, **205**, 1026–1035 (2008).
- [34] Ayuela A, Enkovaara J, and Nieminen R M, Ab initio study of tetragonal variants in Ni<sub>2</sub>MnGa alloy *Journal of Physics: Condensed Matter*, **14**, 5325 – 5336 (2002).

- [35] Brezko T, Barkaline V V, Grechishkin R M, Nelayev V V, *Material Physics and Mechanics*, **9**, 53-67 (2010).
- [36] Tellinen, Suorsa, A Jääskeläinen, Aaltio, Ullakko, *Basic Properties of Magnetic Shape Memory Actuators*, 8th international conference ACTUATOR 2002, Bremen, Germany, (2002).
- [37] Jun Lu, WanchunQu, Chen Wang, *Sensing Characteristics of Magnetic Shape Memory Materials*, *Intelligent Computation Technology and Automation (ICICTA)*, 924–927 (2009).
- [38] KaramanBasaran B, Karaca H E, Karsilayan A, Chumlyakov, *Energy harvesting using martensite variant reorientation mechanism in NiMnGa magnetic shape memory alloy*, *Applied physics letters*, **90**, 172505-508 (2007).
- [39] ManickamMahendran, Jorge Feuchtwanger and Robert C, O’Handley, *Acoustic Energy Absorption in Ferromagnetic Ni-Mn-Ga Shape Memory Alloy Polymer Composites*, *Advanced Materials Research* **52**, 87-94 (2008).
- [40] David C Dunand, Peter Müllner, *Size Effects on Magnetic Actuation in Ni-Mn-Ga Shape-Memory Alloys*, *Advanced Materials*, **23**, Issue 2, 216–232 (2011).
- [41] [www.comp.chem.umn.edu/mn-gsm/dft.pdf](http://www.comp.chem.umn.edu/mn-gsm/dft.pdf)
- [42] Parr R G, Yang W, *Density Functional Theory of atoms and molecules*, Oxford (1989).
- [43] Frisch MJ, Trucks GW, Schlegel HB, Scuseria GE, Robb MA, Cheeseman JR, Montgomery Jr JA, Vreven T, Kudin KN, Burant JC, Millam JM, Iyengar SS, Tomasi J, Barone V, Mennucci B, Cossi M, Scalmani G, Rega N, Petersson GA, Nakatsuji H, Hada M, Ehara M, Toyota K, Fukuda R, Hasegawa J, Ishida M, Nakajima T, Honda Y, Kitao O, Nakai H, Klene M, Li X, Knox JE, Hratchian HP, Cross JB, Bakken V, Adamo C, Jaramillo J, Gomperts R, Stratmann RE, Yazyev O, Austin AJ, Cammi R, Pomelli C, Ochterski JW, Ayala PY, Morokuma K, Voth GA, Salvador P, Dannenberg



JJ, Zakrzewski VG, Dapprich S, Daniels AD, Strain MC, Farkas O, Malick DK, Rabuck AD, Raghavachari K, Foresman JB, Ortiz JV, Cui Q, Baboul AG, Clifford S, Cioslowski J, Stefanov BB, Liu G, Liashenko A, Piskorz P, Komaromi I, Martin RL, Fox DJ, Keith T, Al-Laham MA, Peng CY, Nanayakkara A, Challacombe M, Gill PMW, Johnson B, Chen W, Wong MW, Gonzalez C, Pople JA (2004) Gaussian 03. Gaussian Inc, Wallingford CT.

- [44] Kraus W, Nolze G (BAM Berlin), PowderCell 2.4, Federal Institute of Materials Research and Testing, 87, D-12205, Berlin, (2010).
- [45] Frisch A, Neilson A B, Holder A J, Gaussview user Manual, Gaussian Incorporated, Pittsburgh, PA (2000).
- [46] [www.gausssum.sourceforge.net](http://www.gausssum.sourceforge.net).
- [47] [www.Chemcraft.com](http://www.Chemcraft.com).
- [48] [www.gabedit.sourceforge.net](http://www.gabedit.sourceforge.net).
- [49] Barman S R, AparnaChakrabarti, Sanjay Singh, Banik, Bhardwaj, Paulose, Chalke, Panda, Mitra, Awasthi, Theoretical prediction and experimental study of a ferromagnetic shape memory alloy: Ga<sub>2</sub>MnNi, Physical Review B, **78**, 134406 -1-6 (2008).
- [50] Peter Larkin, Infrared and Raman spectroscopy, Principles and Spectral Interpretation, Boston, Ch2, pgs 7-20 (2011).
- [51] Barbara Start, Infrared Spectroscopy , Fundamentals and Applications Analytical Techniques in the Science , John Wiley & Sons , Ch3, pgs 45-55 (2004).
- [52] Alexey T Zayak, A first-principles investigation of the magnetic, structural and dynamical properties of Ni-Mn-Ga, Doctoral Thesis, (2003).

- [53] LucioFrydman, Encyclopaedia of Nuclear Magnetic Resonance, Fundamentals of Multiple-Quantum Magic-Angle Spinning NMR on Half-Integer Quadrupolar Nuclei **9**, 262–274 (2002).
- [54] Lara Righi, Franca Albertini, GianlucaCalestani, Luigi Pareti, Antonio Paoluzi, Clemens Ritter, Pedro A Algarabel, Luis Morellon, M Ricardo Ibarra, Incommensurate modulated structure of the ferromagnetic shape-memory Ni<sub>2</sub>MnGa martensite, Journal of Solid State Chemistry, **179**, 3525–3533 (2006).
- [55] Chengbao Jiang, Gen Feng, Shengkai Gong, HuibinXu, Effect of Ni Excess on Phase Transformation Temperatures of NiMnGa Alloys,Material Science Engineering A, **342**, 231-235 (2003).
- [56] Wang H B, Chen F, Gao Z Y, Cai W, Zhao L C, Effect of Fe content on fracture behavior of Ni–Mn–Fe–Ga ferromagnetic shape memory alloys, Material Science Engineering A, **438**, 990-993 (2006).
- [57] Gaitzsch U, Potschke M, Roth S, Rellinghaus B, Schultz L, A 1% magnetostrain in polycrystalline 5M Ni–Mn–Ga, ActaMaterialia, **57**, 365-367 (2009).

## List of Publications

1. Shanmugasundari R and Manickam Mahendran, Theoretical study of structure and properties of Ni<sub>2</sub>MnGa Heusler alloy, International Journal of Current Research, Vol. 3, Issue 11, 286-291, (2011).
2. Shanmugasundari R and Manickam Mahendran, Theoretical Study of Ni<sub>2</sub>MnGa Heusler alloy, 56<sup>th</sup> DAE - Solid State Physics Symposium , AIP Proc. India, pp.238, (2012).
3. Shanmugasundari R, Vallalperuman K, Seenithurai S, Chokkalingam R, Senthur Pandi R, Kodipandian R, Manickam Mahendran, Structural and magnetic properties of Ni-Mn-Ga: A DFT study, Proc. of the Conference on Magnetic Materials and Applications, Thiagarajar College of Engineering, pp 147, (2010).
4. Shanmugasundari R and Manickam Mahendran, Study of Ni-Mn-Ga Using Computational Methods, Proc. of the International Conference on Mathematics in Engineering & Business Management, pp.150-153, (2012).
5. Shanmugasundari R and Manickam Mahendran, Density Functional Theoretical Study of the Electronic Structure of Ni-Mn-Ga, Proc. of the Conference on Magnetic Materials and Applications, IIT Madras, Chennai, pp.58, (2012).
6. Shanmugasundari R and Manickam Mahendran, Theoretical NMR spectral study of Ni-Mn-Ga, Communicated to International Journal of Material Engineering, (2012).
7. Shanmugasundari R and Manickam Mahendran, Theoretical IR spectral study of Ni-Mn-Ga, to be communicated to International Journal of Material Science, (2012).